C. R. Geoscience 351 (2019) 141–146

Contents lists available at ScienceDirect

Comptes Rendus Geoscience

www.sciencedirect.com

Internal Geophysics

Effects of Fe and Al incorporations on the bridgmanite–postperovskite coexistence domain

Xianlong Wang [a,b,*], Taku Tsuchiya [c,d,**], Zhi Zeng [a,b]

[a] Key Laboratory of Materials Physics, Institute of Solid State Physics, Chinese Academy of Sciences, Hefei 230031, China
[b] University of Science and Technology of China, Hefei 230026, China
[c] Geodynamics Research Center, Ehime University, Ehime 790-8577, Japan
[d] Earth-Life Science Institute, Tokyo Institute of Technology, Tokyo 152-8550, Japan

ARTICLE INFO

Article history:
Received 6 February 2018
Accepted after revision 25 October 2018
Available online 23 December 2018

Handled by Guillaume Fiquet

Keywords:
Bridgmanite
Postperovskite transition
D″ seismic discontinuities
First-principle simulations

ABSTRACT

The postperovskite phase transition of Fe and Al-bearing $MgSiO_3$ bridgmanite, the most aboundant mineral in the Earth's lower mantle, is believed to be a key to understanding seismological observations in the D″ layer, e.g., the discontinuous changes in seismic wave velocities. Experimentally reported phase transition boundaries of Fe and Al-bearing bridgmanite are currently largely controversial and generally suggest wide two-phase coexistence domains. Theoretical simulations ignoring temperature effects cannot evaluate correctly two-phase coexistence domains under high-temperature. We show high-pressure and high-temperature phase transition boundaries for various compositions with geophysically relevant impurities of $Fe^{2+}SiO_3$, $Fe^{3+}Fe^{3+}O_3$, $Fe^{3+}Al^{3+}O_3$, and $Al^{3+}Al^{3+}O_3$ derived from the ab initio finite-temperature free energies calculated combining the internally consistent LSDA + U method and a lattice dynamics approach. We found that at ~2500 K, incorporations accompanied by Fe^{3+} expand the two-phase coexistence domains distinctly, implying that D″ seismic discontinuities likely arise from the phase transition of Fe^{2+}-bearing bridgmanite.

The postperovskite (PPv) phase transition of bridgmanite (Brg), which is the most abundant lower mantle mineral (Poirier, 1991; Wang et al., 2015), occurs at the pressure (P), temperature (T) conditions (Murakami et al., 2004; Tsuchiya et al., 2004) close to the Earth's D″ layer located between the silicate lower mantle and the metallic outer core. Therefore, it is quite likely that PPv is the most dominant mineral in the D″ layer and that the PPv phase transition of Brg is responsible for the discontinuous increase in shear wave velocity in this region (Garnero and McNamara, 2008; Hutko et al., 2008; Lay, 2008; Lay et al., 1998; van der Hilst et al., 2007). In the lower mantle, Brg forms a solid solution with $Fe^{2+}SiO_3$, $Fe^{3+}Fe^{3+}O_3$, $Fe^{3+}Al^{3+}O_3$, and $Al^{3+}Al^{3+}O_3$ (Kesson et al., 1998; McCammon, 1997). This produces the Brg + PPv two-phase coexistence (TPC) domain, whose width changes depending on the type and amount of solute. To understand the relationship between the PPv phase transition and the D″ seismic discontinuities, it is critical to clarify the effects of solutes on the TPC domain of the PPv phase transition.

* Corresponding author at: Key Laboratory of Materials Physics, Institute of Solid State Physics, Chinese Academy of Sciences, Hefei 230031, China.
** Co-corresponding author at: Geodynamics Research Center, Ehime University, Ehime 790-8577, Japan.
E-mail addresses: xlwang@theory.issp.ac.cn (X. Wang), tsuchiya.taku.mg@ehime-u.ac.jp (T. Tsuchiya).

https://doi.org/10.1016/j.crte.2018.10.003
1631-0713/

However, precise experimental determinations of the multicomponent phase transition boundaries at the core-mantle boundary (CMB) *P,T* (~136 GPa and 2500 ~ 4000 K) (Poirier, 1991) are still challenging (Andrault et al., 2010; Catalli et al., 2009; Grocholski et al., 2012; Hirose and Sinmyo, 2006; Mao et al., 2004; Nishio-Hamane et al., 2007; Sun et al., 2018; Tateno et al., 2005). Previous results, not only on the phase transition pressures but on the width of TPC domains, are largely controversial, e.g., at ~2500 K, Brg with ~10 mol% $Fe^{2+}SiO_3$ was reported to have a TPC domain from 99 GPa to 118 GPa with a ~19 GPa width (Mao et al., 2004), while higher transition pressures with a broader TPC domain from 110 GPa to 134 GPa with a ~24 GPa width (Catalli et al., 2009) were also proposed. Furthermore, the phase transitions of 10 mol% and 15 mol% $Fe^{3+}Al^{3+}O_3$-bearing Brg under 2500 K were reported to 111 GPa and 147 GPa with TPC widths of ~22 GPa and ~26 GPa, respectively (Catalli et al., 2009; Nishio-Hamane et al., 2007). A similar controversy can also be seen in experiments on more complicated multi-phase aggregates (Grocholski et al., 2012; Murakami et al., 2005). Generally, experimental measurements presented broad TPC domains notably larger than the typical seismic detection limit of 5 GPa (~80 km in depth) (Lay and Garnero, 2007), since the seismic body waves with a typical frequency of ~1 Hz have this scale of wavelengths. Also, in some experiments, the PPv transition was detected to start at pressures higher than the CMB pressure of 136 GPa (Tateno et al., 2005). These indicate that the discontinuities in the D″ layer might not arise from the PPv phase transition of Brg.

Computational simulations based on the first-principles method, which can theoretically explore the material properties relying only on basic physical laws, were also carried out to investigate the PPv phase transition behaviors of Fe and Al-bearing Brg (Akber-Knutson et al., 2005; Caracas and Cohen, 2005, 2008; Metsue and Tsuchiya, 2012; Tsuchiya and Tsuchiya, 2008; Zhang and Oganov, 2006). The general conclusion drawn from these previous studies is that the Fe and Al incorporations decrease and increase the transition pressure, respectively. However, theoretical simulations carried out at static condition ignoring the lattice thermal effects (Akber-Knutson et al., 2005; Caracas and Cohen, 2005, 2008; Zhang and Oganov, 2006) give unreasonable TPC ranges. In addition, the strongly correlated interactions among the Fe 3d orbitals that must be treated correctly for the Fe-bearing cases were not considered (Akber-Knutson et al., 2005; Caracas and Cohen, 2008; Zhang and Oganov, 2006). By means of the method we developed (Metsue and Tsuchiya, 2012; Tsuchiya and Wang, 2013; Wang et al., 2015), the high-*P,T* properties of Brg containing geophysically relevant solute elements can be directly simulated with an appropriate treatment by the internally consistent Hubbard *U* correction. Based on the thermoelasticity of Fe and Al-bearing Brg investigated by this technique, it was recently reported that the pyrolite model containing ~80 vol% Brg and ~20 vol% ferropericlase (Fe-bearing MgO) is reasonable for the average lower mantle composition (Wang et al., 2015). Also using the same technique, it was suggested that at ~2500 K, the PPv phase transition with 6.25 mol% $Fe^{2+}SiO_3$ and $Al^{3+}Al^{3+}O_3$ acquires relatively narrow TPC ranges (Caracas and Cohen, 2008; Metsue and Tsuchiya, 2012). However, effects of the Fe^{3+}, which are also expected to be important in the lower mantle (Kesson et al., 1998; McCammon, 1997), on the TPC domain still remain unexplored. In this work, we systematically study the effects of $Fe^{2+}SiO_3$, $Fe^{3+}Fe^{3+}O_3$, $Fe^{3+}Al^{3+}O_3$, and $Al^{3+}Al^{3+}O_3$ incorporations on the PPv phase transition boundary under high *T*.

We reported the structures, spin states, and thermodynamic properties of $Fe^{2+}SiO_3$, $Fe^{3+}Fe^{3+}O_3$, $Fe^{3+}Al^{3+}O_3$, and $Al^{3+}Al^{3+}O_3$-bearing Brg in our previous works (Metsue and Tsuchiya, 2012; Tsuchiya and Tsuchiya, 2008; Tsuchiya and Wang, 2013; Wang et al., 2015). For PPv, previous results showed that 12.5 mol% Fe substituted at the Mg and the Si site have the high spin (HS) and the low spin (LS) state in its thermodynamic stability pressure range, respectively (Tsuchiya and Wang, 2013). We studied the stable spin configuration of 6.25 mol% Fe using a PPv supercell containing 80 atoms (fig. S1B), and our results agree with that of 12.5 mol% Fe-bearing cases (Tsuchiya and Wang, 2013) under the high-*P* range (from 50 GPa to 180 GPa). Therefore, we can conclude that within the Fe concentration smaller than ~12.5 mol%, the spin configuration of Fe-bearing PPv is independent of iron concentration (Supplementary Material and Fig. S2). Therefore, phonons of the configurations of $(Mg,Fe^{2+}_{HS})SiO_3$, $(Mg,Fe^{3+}_{HS})(Si,Fe^{3+}_{LS})O_3$ $(Si,Fe^{3+}_{LS})O_3$, $(Mg,Fe^{3+}_{HS})(Si,Al^{3+})O_3$, $(Mg,Al^{3+})(Si,Al^{3+})O_3$ are calculated in this study.

Phonon dispersions are calculated up to 210 GPa, and no imaginary frequency is observed above 70 GPa (fig. S3), indicating that 6.25 mol% Fe and Al-bearing PPv are vibrationally stable from the middle to deep lower mantle, even though thermodynamically unstable. Phonon dispersions and vibrational density of states (VDoS) of $(Mg,Fe^{3+}_{HS})(Si,Al^{3+})O_3$ at 120 GPa are representatively shown in Fig. S3. It is found that Al^{3+} contributes to phonons in the middle broad frequency range (blue line in Fig. S3), whereas Fe^{3+} mainly contributes to phonons in the low acoustic frequency range (red line in fig. S3) due to its heavy mass. The calculated thermal equations of state (EoS) of 6.25 mol% Fe and Al-bearing PPv under 300 K and 2000 K and corresponding thermodynamic parameters are presented in Fig. S4 and Table S1, respectively. Calculated volumes of $(Mg,Fe^{2+}_{HS})SiO_3$ and $(Mg,Fe^{3+}_{HS})(Si,Al^{3+})O_3$ PPv at 300 K agree well with experimental values (Nishio-Hamane et al., 2007; Shieh et al., 2006), as seen in our previous studies of Fe and Al-bearing Brg (Metsue and Tsuchiya, 2012; Tsuchiya and Wang, 2013; Wang et al., 2015), which shows the reliability of our computational techniques. At 2000 K, $(Mg,Fe^{2+}_{HS})SiO_3$ PPv and $(Mg,Al^{3+})(Si,Al^{3+})O_3$ PPv have comparable volumes with pure $MgSiO_3$ PPv, while the volume of $MgSiO_3$ PPv is expanded a little by the incorporation of 6.25 mol% $Fe^{3+}Fe^{3+}O_3$ and $Fe^{3+}Al^{3+}O_3$, e.g., at 120 GPa and 2000 K, the volumes of $(Mg,Fe^{3+}_{HS})(Si,Fe^{3+}_{LS})O_3$ PPv and $(Mg,Fe^{3+}_{HS})(Si,Al^{3+})O_3$ PPv are ~0.60% and ~0.44%, respectively, larger than that of pure $MgSiO_3$ PPv. These small volume differences would be quite difficult to detect experimentally.

Including the zero-point vibrational energy, the calculated phase transition pressure of pure $MgSiO_3$ at 0 K is 95.4 GPa, and it increases up to 115.8 GPa, 121.4 GPa, and 127.0 GPa at 2000 K, 2500 K, and 3000 K, respectively, because of the positive Clapeyron slope of the PPv phase boundary (Murakami et al., 2004; Tsuchiya et al., 2004). As shown in Table S2 at 0 K, the presence of 6.25 mol% $Fe^{2+}SiO_3$ and $Fe^{3+}Fe^{3+}O_3$ decreases the PPv phase transition pressures by 2.5 GPa and 4.3 GPa, respectively. Moreover, the transition pressure of 6.25 mol% $Fe^{3+}Al^{3+}O_3$ ($Al^{3+}Al^{3+}O_3$)-bearing Brg is by 0.5 GPa (3.4 GPa) higher than that of pure $MgSiO_3$. The results indicate that at 0 K, the incorporation of a small amount of Fe and Al, respectively, decreases and increases the transition pressure, which is consistent with previous theoretical works (Akber-Knutson et al., 2005; Caracas and Cohen, 2005, 2008; Tsuchiya et al., 2004; Zhang and Oganov, 2006).

The high-T (from 2000 K to 3000 K) TPC domains determined by finite-temperature free energies (supplementary materials) are shown in Fig. 1 and Table S2 with previous estimations (Akber-Knutson et al., 2005; Andrault et al., 2010; Caracas and Cohen, 2005, 2008; Catalli et al., 2009; Grocholski et al., 2012; Hirose and Sinmyo, 2006; Lay and Garnero, 2007; Metsue and Tsuchiya, 2012; Murakami et al., 2005; Nishio-Hamane et al., 2007; Sun et al., 2018; Tateno et al., 2005; Tsuchiya and Tsuchiya, 2008; Zhang and Oganov, 2006). It can be seen that at 2500 K, the incorporation of 6.25 mol% $Fe^{2+}SiO_3$ slightly decreases the phase transition pressure with a quite narrow TPC domain of ~ 0.8 GPa. This pressure variation corresponds to a thickness of ~ 20 km, which is sufficiently smaller than the typical seismological detection limit of 5 GPa (Lay and Garnero, 2007). The previous simulations also gave a narrow TPC domain of ~ 3.8 GPa for the case of 6.25 mol% Fe^{2+}-bearing $MgSiO_3$ (Caracas and Cohen, 2008), as shown in Table S2. Similarly, a narrow TPC domain of ~ 2.3 GPa is found in the case of 6.25 mol% $Al^{3+}Al^{3+}O_3$-bearing Brg, which is well consistent with our previous work (Tsuchiya and Tsuchiya, 2008). Compared to 0 K, the transition pressure at high-T slightly decreases due to phonon effects (Tsuchiya and Tsuchiya, 2008). In contrast to $Fe^{2+}SiO_3$- and $Al^{3+}Al^{3+}O_3$-bearing cases, results in Fig. 1C and D, demonstrate that the 6.25 mol% $Fe^{3+}Fe^{3+}O_3$ and $Fe^{3+}Al^{3+}O_3$ incorporations expand the Brg + PPv TPC domain significantly in addition to a lowering of the transition pressure. At 2500 K, the coexistence domains of 6.25 mol% $Fe^{3+}Fe^{3+}O_3$- and $Fe^{3+}Al^{3+}O_3$-bearing Brg are 8.8 GPa and 16.8 GPa, respectively, which are much broader than the seismological

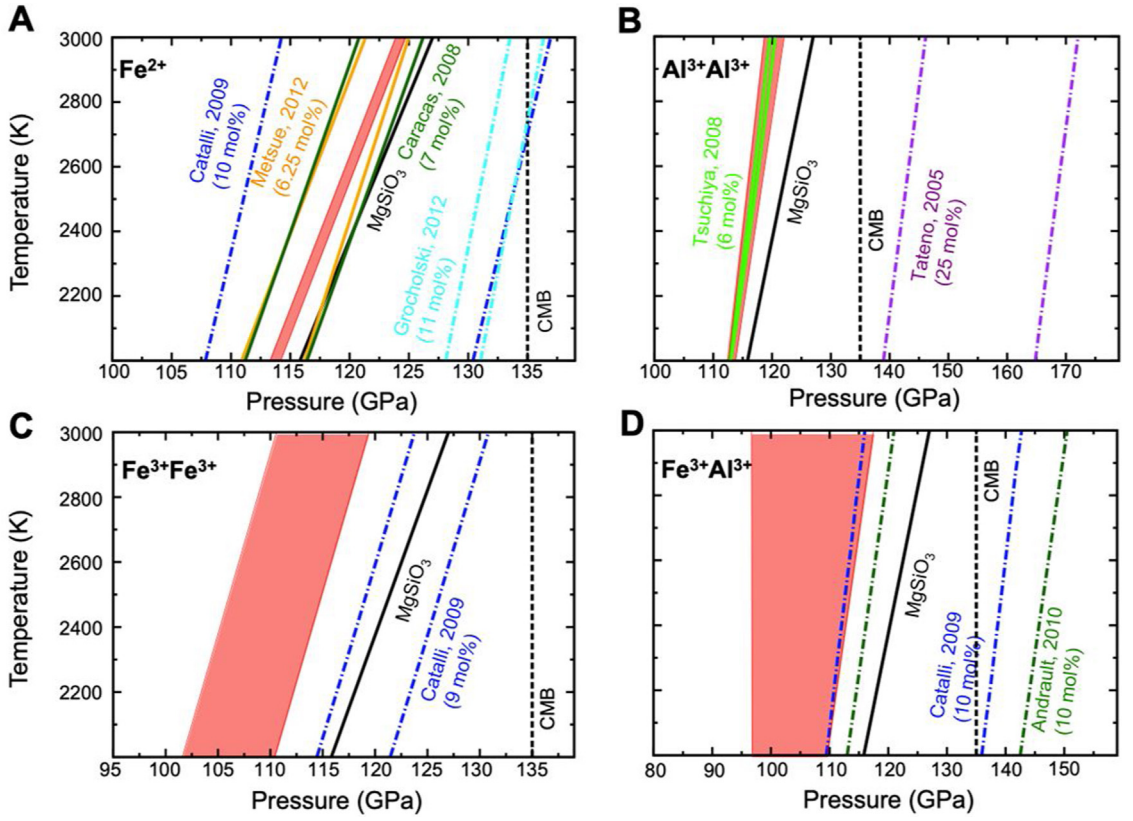

Fig. 1. Two-phase coexistence (TPC) domains of Fe and Al-bearing $MgSiO_3$ at ~ 2500 K. A–D. The TPC domain of $MgSiO_3$ containing 6.25 mol% $Fe^{2+}SiO_3$ (A), $Al^{3+}Al^{3+}O_3$ (B), $Fe^{3+}Fe^{3+}O_3$ (C), and $Fe^{3+}Al^{3+}O_3$ (D). The TPC domains are represented by the red-shaded areas. Vertical black dashed lines indicate the P condition of the CMB, and the phase boundary of pristine $MgSiO_3$ is represented by the black solid line. Experimentally reported TPC domains are shown by colored dotted dashed lines, purple for Tateno et al. (2005), blue for Catalli et al. (2009), dark-green for Andrault et al. (2010), and light-blue for Grocholski et al. (2012). Previous theoretical estimations of TPC domains are shown by solid colored lines, dark-green for Caracas and Cohen (2008), light-green for Tsuchiya and Tsuchiya (2008), and orange for Metsue and Tsuchiya (2012).

detection limit. Please note that the key process of the PPv phase transition is the octahedral tilting and that the octahedral tilting is easier when a smaller ion occupies the Mg site, resulting in a lower phase transition pressure. Therefore, the large differences in the thickness of the TPC domain between Fe^{2+} and Fe^{3+}-bearing Brg are mainly due to the fact that Fe^{2+}(92 pm) has larger ionic radius than Fe^{3+}(78.5 pm), as discussed in the supplementary materials.

In Fig. 2, the TPC domains are shown as a function of solute concentration. At 2500 K, the width of the TPC domain in $(Mg, Fe^{2+}_{HS})SiO_3$ remains narrow, even when the $Fe^{2+}SiO_3$ concentration increases to 16 mol%. Also, the TPC width in $(Mg,Al^{3+})(Si,Al^{3+})O_3$ expands only slightly to ~5 GPa when increasing the $Al^{3+}Al^{3+}O_3$ concentration to ~16 mol%. In contrast, a TPC with a width of 5 GPa is seen in the system only with ~3.3 mol% $Fe^{3+}Fe^{3+}O_3$ and ~1.5 mol% $Fe^{3+}Al^{3+}O_3$, indicating that the D″ seismic discontinuity might arise from the PPv phase transition of Fe^{2+}-bearing Brg, but not from that of Fe^{3+}-bearing Brg. Therefore, the PPv phase transition in the subducted basaltic materials, which generally contains ~20 mol% Al_2O_3 and ~10 mol% FeO (Hirose et al., 2005), is not likely to produce the discontinuous velocity changes atop the D″ layer. Moreover, a subducted basaltic component may induce a strong chemical contrast in the environments of pyrolytic-type lower mantle, which may lead to a sharp change in seismic properties. We will investigate this topic in the following work. Several experiments suggested that, even in the pyrolitic mineral aggregates, Fe^{3+} becomes more abundant (~70%) in Brg than Fe^{2+} under lower mantle conditions with the co-incorporation of ~6 mol% Al (Kesson et al., 1998), independently of oxygen fugacity (Nakajima et al., 2012). In addition, some works reported that a higher Fe^{2+} ratio was observed at the midmantle pressure range (40–70 GPa), while Fe^{3+} became dominant at pressures above 70 GPa (Andrault et al., 2018; Shim et al., 2017). The present results demonstrate that the PPv transition in such Brg has a wide TPC domain of ~17.5 GPa, indicating that the sharp change in any physical property is hard to be expected across the PPv phase transition, even in the pyrolitic composition. Therefore, other origins of the D″ discontinuity are solicited, such as the compositional boundary (McNamara and Zhong, 2005) by assuming accumulations of high-velocity materials on the bottom of the mantle.

Our simulations, however, clearly show that the PPv phase transition in Fe^{2+}-bearing Brg accompanies the narrow TPC domain, which may can be detected by seismological observations. Al-free or poor Brg is rather known to be produced in depleted peridotite such as harzburgite, which composes the most part of the subducted slabs (Irifune and Ringwood, 1987). It is therefore strongly suggested that places beneath circum-Pacific, where the positive shear wave discontinuities are observed, have a high concentration in depleted materials.

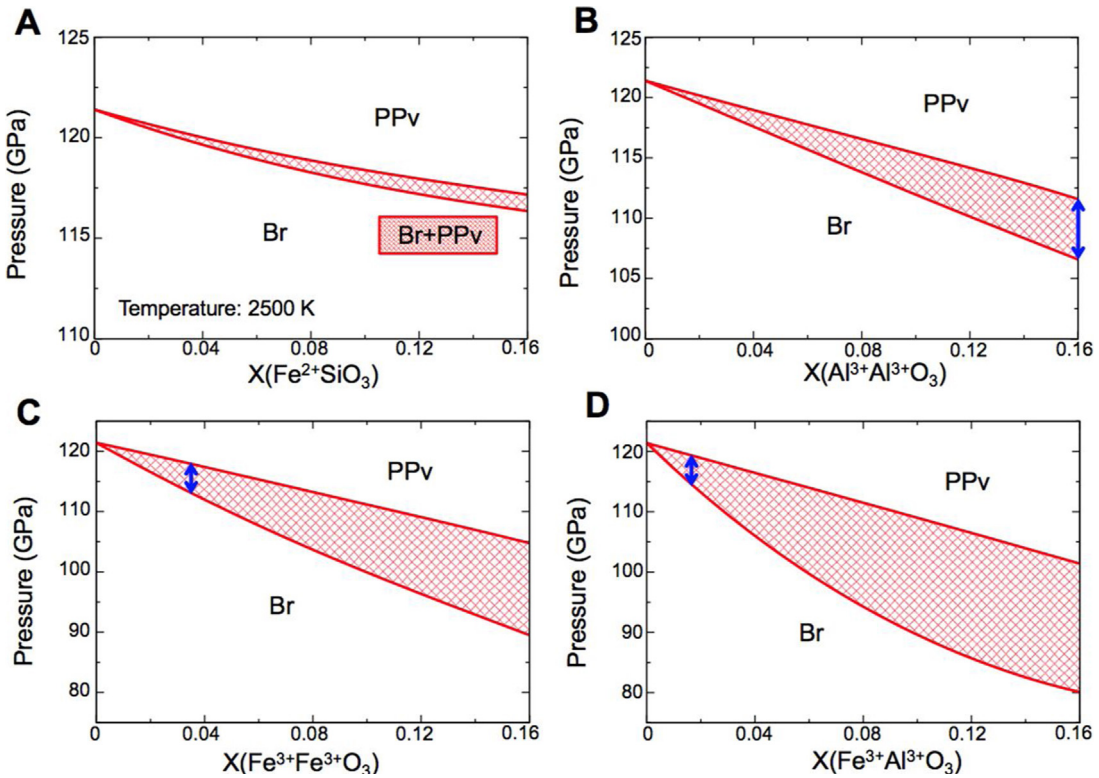

Fig. 2. Phase diagrams of Fe and Al-bearing $MgSiO_3$ at 2500 K. A. Phase diagram of the $MgSiO_3$–$Fe^{2+}SiO_3$ binary system. B. Phase diagram of the $MgSiO_3$-$Al^{3+}Al^{3+}O_3$ binary system. C. Phase diagram of the $MgSiO_3$–$Fe^{3+}Fe^{3+}O_3$ binary system. D. Phase diagram of the $MgSiO_3$-$Fe^{3+}Al^{3+}O_3$ binary system. The two-phase coexistence (TPC) domains are shown by red mesh areas. The blue arrows indicate the pressure width of TPC domains equal to 5 GPa.

This is consistent with the fact that the circum-Pacific comprises the most active subduction zones. Also, there would be another possibility that these regions are related to geochemically assumed early depleted reservoir (Boyet and Carlson, 2005, 2006). In contrast, the D″ discontinuities are not so distinct beneath central Pacific and Africa, where the large low-S velocity (LLSV) anomalies are observed instead (Lay and Garnero, 2007). In the edges of LLSV provinces, there are some ultra-low-velocity zones (ULVZs), where the compressional and shear wave velocities are 5–10% and 10–30% smaller than that of surrounding minerals. The low-V_S bodies are often discussed associated with accumulations of subducted basaltic materials (McNamara and Zhong, 2005). Since they are expected to contain a large amount of Fe^{3+}, Brg in those regions hardly produces a sharp PPv transition. This view is highly consistent with no or rare observations of the D″ discontinuity in the LLSV provinces (Lay and Garnero, 2007). The present large scale ab initio computations integrating several advanced techniques of direct lattice dynamics, quasi-harmonic approximation, and internally consistent LDA + U therefore suggest a heterogenous distribution of depleted and fertile materials in the D″ layer, which would be formed as a result of the global mantle circulation.

Acknowledgements

We thank D.Y. Sun for helpful comments and S. Whitaker for support to the preparation of the manuscript. This research was supported by the NSFC under Grant 11674329 and U1230202 (NSAF) and MEXT/JSPS KAKENHI JP20001005, JP21740379, and JP15H05834.

Appendix A. Supplementary data

Supplementary data associated with this article can be found, in the online version, at https://doi.org/10.1016/j.crte.2018.10.003.

References

Akber-Knutson, S., Steinle-Neumann, G., Asimow, P.D., 2005. Effect of Al on the sharpness of the $MgSiO_3$ perovskite to postperovskite phase transition. Geophys. Res. Lett. 32, L14303.

Andrault, D., Muñoz, M., Bolfan-Casanova, N., Guignot, N., Perrillat, J.-P., Aquilanti, G., Pascarelli, S.D., 2010. Experimental evidence for perovskite and postperovskite coexistence throughout the whole D″ region. Earth Planet. Sci. Lett. 293, 90–96.

Andrault, D., Munoz, M., Pesce, G., Cerantola, V., Chumakov, A., Kantor, I., Pascarelli, S., Ruffer, R., Hennet, L., 2018. Large oxygen excess in the primitive mantle could be the source of the great oxygenation Event. Geochem. Perspect. Lett. 6, 5–10.

Boyet, M., Carlson, R.W., 2005. ^{142}Nd evidence for early (> 4.53 Ga) global differentiation of the silicate earth. Science 309, 576–581.

Boyet, M., Carlson, R.W., 2006. A new geochemical model for the Earth's mantle inferred from ^{146}Sm–^{142}Nd systematics. Earth Planet. Sci. Lett. 250, 254–268.

Caracas, R., Cohen, R.E., 2005. Effect of chemistry on the stability and elasticity of the perovskite and postperovskite phases in the $MgSiO_3$–$FeSiO_3$–Al_2O_3 system and implications for the lowermost mantle. Geophys. Res. Lett. 32, L16310.

Caracas, R., Cohen, R.E., 2008. Ferrous iron in postperovskite from first-principles calculations. Phys. Earth Planet. Inter. 168, 147–152.

Catalli, K., Shim, S.-H., Prakapenka, V., 2009. Thickness and Clapeyron slope of the postperovskite boundary. Nature 462, 782–785.

Garnero, E.J., McNamara, A.K., 2008. Structural and dynamics of Earth's lower mantle. Science 320, 626–628.

Grocholski, B., Catalli, K., Shim, S., Prakapenka, V., 2012. Mineralogical effects on the detectability of the postperovskite boundary. Proc. Natl. Acad. Sci. U S A 109, 2275–2279.

Hirose, K., Sinmyo, R., 2006. Determination of postperovskite phase transition boundary in $MgSiO_3$ using Au and MgO pressure standards. Geophys. Res. Lett. 33, L01310.

Hirose, K., Takafuji, N., Sata, N., Ohishi, Y., 2005. Phase transition and density of subducted MORB crust in the lower mantle. Earth Planet. Sci. Lett. 237, 239–251.

Hutko, A.R., Lay, T., Revenaugh, J., Garnero, E.J., 2008. Anticorrelated seismic velocity anomalies from postperovskite in the lowermost mantle. Science 320, 1070–1074.

Irifune, T., Ringwood, A.E., 1987. Phase transformations in a harzburgite composition to 26 GPa: implications for dynamical behaviour of the subducting slab. Earth Planet. Sci. Lett. 86, 365–376.

Kesson, S.E., Fitz Gerald, J.D., Shelley, J.M., 1998. Mineralogy and dynamics of a pyrolite lower mantle. Nature 393, 252–255.

Lay, T., 2008. Sharpness of the D″ discontinuity beneath the Cocos Plate: implications for the perovskite to postperovskite phase transition. Geophys. Res. Lett. 35, L03304.

Lay, T., Garnero, E.J., 2007. Reconciling the postperovskite phase with seismological observations of lowermost mantle structure. In: Hirose, K., et al. (Eds.), Postperovskite: The Last Mantle Phase Transition. Geophys. Monogr., vol. 174, AGU, Washington, DC, pp. 129–153.

Lay, T., Williams, Q., Garnero, E.J., 1998. The core-mantle boundary layer and deep Earth dynamics. Nature 392, 461–468.

Mao, W.L., Shen, G.Y., Prakapenka, V.B., Meng, Y., Campbell, A.J., Heinz, D.L., Shu, J.F., Hemley, R.J., Mao, H.K., 2004. Ferromagnesian postperovskite silicates in the D″ layer of the Earth. Proc. Natl. Acad. Sci. U S A 101, 15867–15869.

McCammon, C., 1997. Perovskite as a possible sink for ferric iron in the lower mantle. Nature 387, 694–696.

McNamara, A.K., Zhong, S., 2005. Thermochemical structures beneath Africa and the Pacific Ocean. Nature 437, 1136–1139.

Metsue, A., Tsuchiya, T., 2012. Thermodynamic properties of (Mg,Fe^{2+})-SiO_3 perovskite at the lower mantle pressures and temperatures: an internally consistent LSDA + U study. Geophys. J. Int. 190, 310–322.

Murakami, M., Hirose, K., Kawamura, K., Sata, N., Ohishi, Y., 2004. Postperovskite phase transition in $MgSiO_3$. Science 80, 855–858.

Murakami, M., Hirose, K., Sata, N., Ohishi, Y., 2005. Postperovskite phase transition and mineral chemistry in the pyrolitic lowermost mantle. Geophys. Res. Lett. 32, L03304.

Nakajima, Y., Frost, D.J., Rubie, D.C., 2012. Ferrous iron partitioning between magnesium silicate perovskite and ferropericlase and the composition of perovskite in the Earth's lower mantle. J. Geophys. Res. 117, B08201.

Nishio-Hamane, D., Fujino, K., Seto, Y., Nagai, T., 2007. Effect of the incorporation of $FeAlO_3$ into $MgSiO_3$ perovskite on the postperovskite transition. Geophys. Res. Lett. 34, L2307.

Poirier, J.-P., 1991. Introduction to the Physics of the Earth's Interior. Cambridge University Press, Cambridge, England.

Shieh, S.R., Duffy, T.S., Kubo, A., Shen, G.Y., Prakapenka, V.B., Sata, N., Hirose, K., Ohishi, Y., 2006. Equation of state of the postperovskite phase synthesized from a natural $(Mg,Fe)SiO_3$ orthopyroxene. Proc. Natl. Acad. Sci. U S A 103, 3039–3043.

Shim, S.H., Grocholski, B., Ye, Y., Ercan Alp, E., Xu, S.Z., Morgan, D., Meng, Y., Prakapenka, V.B., 2017. Stability of ferrous iron-rich bridgmanite under reducing midmantle conditions. Proc. Natl. Acad. Sci. U S A 114, 6468–6473.

Sun, N.Y., Wei, W., Han, S.J., Song, J.H., Li, X.Y., Duan, Y.F., Prakapenka, V.B., Mao, Z., 2018. Phase transition and thermal equations of state of (Fe,Al)-bridgmanite and postperovskite: Implication for the chemical heterogeneity at the lowermost mantle. Earth Planet. Sci. Lett. 490, 161–169.

Tateno, S., Hirose, K., Sata, N., Ohishi, Y., 2005. Phase relations in $Mg_3Al_2Si_3O_{12}$ to 180 GPa: effect of Al on postperovskite phase transition. Geophys. Res. Lett. 32, L15306.

Tsuchiya, J., Tsuchiya, T., 2008. Postperovskite phase equilibria in the $MgSiO_3$-Al_2O_3 system. Proc. Natl. Acad. Sci. U S A 105, 19160–19164.

Tsuchiya, T., Tsuchiya, J., Umemoto, K., Wentzcovitch, R.M., 2004. Phase transition in $MgSiO_3$ perovskite in the Earth's lower mantle. Earth Planet. Sci. Lett. 224, 241–248.

Tsuchiya, T., Wang, X., 2013. Ab initio investigation on the high-temperature thermodynamic properties of Fe^{3+}-bearing $MgSiO_3$ perovskite. J. Geophys. Res. Solid Earth 118, 83–91.

van der Hilst, R.D., de Hoop, M.V., Wang, P., Shim, S.H., Ma, P., Tenorio, L., 2007. Seismostratigraphy and thermal structure of Earth's core-mantle boundary region. Science 315, 1813–1817.

Wang, X.L., Tsuchiya, T., Hase, A., 2015. Computational support for a pyrolitic lower mantle containing ferric iron. Nat. Geosci. 8, 556–559.

Zhang, F., Oganov, A.R., 2006. Mechanism of Al^{3+} incorporation in $MgSiO_3$ postperovskite at high-pressures. Earth Planet. Sci. Lett. 248, 69–76.